

# Nitrous oxide reduction by two partial denitrifying bacteria requires denitrification intermediates that cannot be resired

Breah LaSarre,<sup>1</sup> Ryan Morlen,<sup>2</sup> Gina C. Neumann,<sup>1</sup> Caroline S. Harwood,<sup>2</sup> James B. McKinlay<sup>1</sup>

**AUTHOR AFFILIATIONS** See affiliation list on p. 14.

**ABSTRACT** Denitrification is a form of anaerobic respiration wherein nitrate ( $\text{NO}_3^-$ ) is sequentially reduced via nitrite ( $\text{NO}_2^-$ ), nitric oxide, and nitrous oxide ( $\text{N}_2\text{O}$ ) to dinitrogen gas ( $\text{N}_2$ ) by four reductase enzymes. Partial denitrifying bacteria possess only one or some of these four reductases and use them as independent respiratory modules. However, it is unclear if partial denitrifiers sense and respond to denitrification intermediates outside of their reductase repertoire. Here, we tested the denitrifying capabilities of two purple nonsulfur bacteria, *Rhodopseudomonas palustris* CGA0092 and *Rhodobacter capsulatus* SB1003. Each had denitrifying capabilities that matched their genome annotation; CGA0092 reduced  $\text{NO}_2^-$  to  $\text{N}_2$ , and SB1003 reduced  $\text{N}_2\text{O}$  to  $\text{N}_2$ . For each bacterium,  $\text{N}_2\text{O}$  reduction could be used both for electron balance during growth on electron-rich organic compounds in light and for energy transformation via respiration in darkness. However,  $\text{N}_2\text{O}$  reduction required supplementation with a denitrification intermediate, including those for which there was no associated denitrification enzyme. For CGA0092,  $\text{NO}_3^-$  served as a stable, non-catalyzable molecule that was sufficient to activate  $\text{N}_2\text{O}$  reduction. Using a  $\beta$ -galactosidase reporter, we found that  $\text{NO}_3^-$  acted, at least in part, by stimulating  $\text{N}_2\text{O}$  reductase gene expression. In SB1003,  $\text{NO}_2^-$  but not  $\text{NO}_3^-$  activated  $\text{N}_2\text{O}$  reduction, but  $\text{NO}_2^-$  was slowly removed, likely by a promiscuous enzyme activity. Our findings reveal that partial denitrifiers can still be subject to regulation by denitrification intermediates that they cannot use.

**IMPORTANCE** Denitrification is a form of microbial respiration wherein nitrate is converted via several nitrogen oxide intermediates into harmless dinitrogen gas. Partial denitrifying bacteria, which individually have some but not all denitrifying enzymes, can achieve complete denitrification as a community by cross-feeding nitrogen oxide intermediates. However, the last intermediate, nitrous oxide ( $\text{N}_2\text{O}$ ), is a potent greenhouse gas that often escapes, motivating efforts to understand and improve the efficiency of denitrification. Here, we found that at least some partial denitrifying  $\text{N}_2\text{O}$  reducers can sense and respond to nitrogen oxide intermediates that they cannot otherwise use. The regulatory effects of nitrogen oxides on partial denitrifiers are thus an important consideration in understanding and applying denitrifying bacterial communities to combat greenhouse gas emissions.

**KEYWORDS** denitrification, nitrous oxide, anaerobic respiration, photoheterotrophy, purple nonsulfur bacteria, *Rhodopseudomonas*, *Rhodobacter*, greenhouse gas, nitrate, nitrite

**D**enitrification is a multistep respiratory pathway that sequentially reduces nitrate ( $\text{NO}_3^-$ ) via nitrite ( $\text{NO}_2^-$ ), nitric oxide (NO), and nitrous oxide ( $\text{N}_2\text{O}$ ) to dinitrogen gas ( $\text{N}_2$ ) (1, 2) (Fig. 1A). Denitrifying bacteria are important in several contexts. Denitrifiers in the human gut help fight pathogens and maintain vascular homeostasis through the generation of  $\text{NO}_2^-$  and NO (3). Denitrification is also important to the global

**Editor** Arpita Bose, Washington University, St. Louis, Missouri, USA

Address correspondence to James B. McKinlay, jmckinla@indiana.edu.

The authors declare no conflict of interest.

See the funding table on p. 14.

**Received** 4 October 2023

**Accepted** 4 November 2023

**Published** 11 December 2023

Copyright © 2023 American Society for Microbiology. All Rights Reserved.

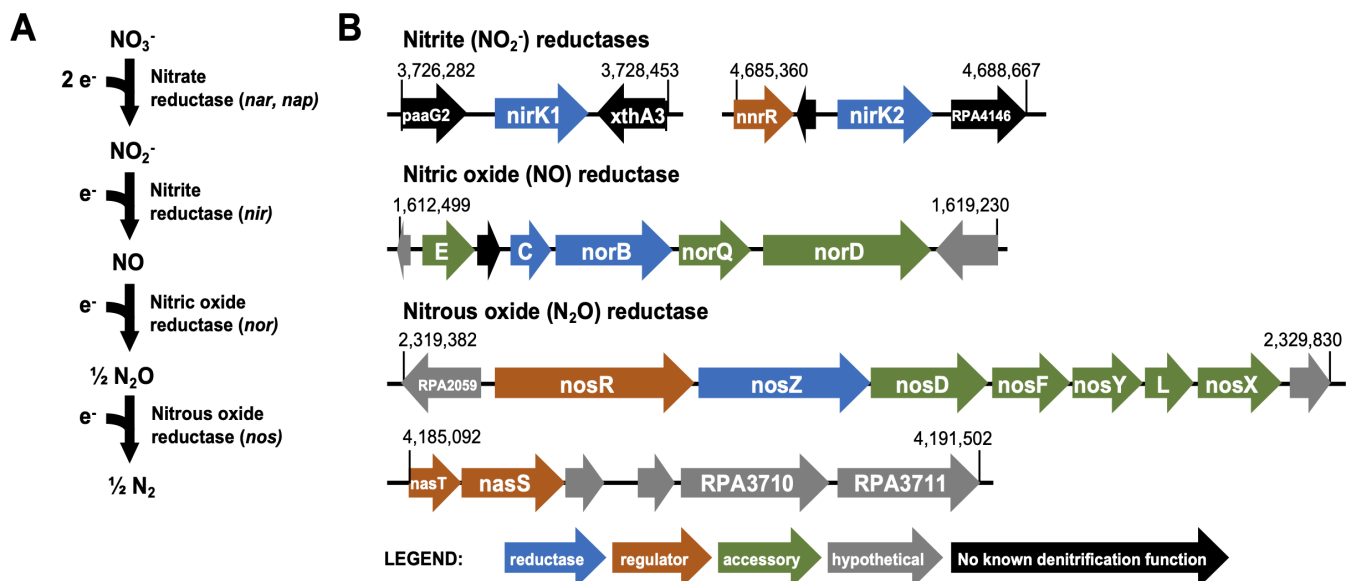


**FIG 1** General denitrification pathway (A) and denitrification genes annotated in *R. palustris* CGA0092 (B). Numbers indicate the chromosome nucleotide positions. Several CRP/Fnr family transcriptional regulators with >25% sequence identity to known denitrification regulators are not shown.

nitrogen cycle, returning nitrogen to the atmosphere as  $\text{N}_2$ . However,  $\text{N}_2\text{O}$  often escapes denitrifying communities before it can be reduced to  $\text{N}_2$ .  $\text{N}_2\text{O}$  is a potent greenhouse gas and also damages the ozone layer (4).  $\text{N}_2\text{O}$  emissions have increased to concerning levels, primarily due to transformation of  $\text{NO}_3^-$  in agricultural fertilizers to  $\text{N}_2\text{O}$  by naturally occurring denitrifying bacteria in the soil (5, 6). Thus, there is a need to better understand and improve the efficiency of denitrification.

Many bacteria lack a complete denitrification pathway and are thus called partial or truncated denitrifiers (7–11). Partial denitrifiers use single or multiple steps of the pathway as independent respiratory modules (1, 2). Although incapable of reducing  $\text{NO}_3^-$  to  $\text{N}_2$  on their own, partial denitrifiers are important contributors to complete denitrification as a community process, with intermediates cross-fed between community members that have different segments of the pathway (7–12). Notably, nitrogen oxides ( $\text{NO}_3^-$ ,  $\text{NO}_2^-$ ,  $\text{NO}$ , or  $\text{N}_2\text{O}$ ) not only serve as substrates for denitrification reductases but also act as regulators of denitrification. Although regulatory roles have been well characterized in bacteria capable of complete denitrification, regulatory roles in partial denitrifiers have received comparatively less attention. In particular, it is unclear if the regulatory effects of nitrogen oxides in partial denitrifiers match their reductase repertoire.

Here, we characterized the ability of two purple non-sulfur bacteria (PNSB) that are putative partial denitrifiers, *Rhodopseudomonas palustris* CGA0092 and *Rhodobacter capsulatus* SB1003, to carry out denitrification under phototrophic and chemoheterotrophic conditions. Under phototrophic conditions, where light is the energy source, we tested if nitrogen oxides can serve as an essential electron acceptor to maintain electron balance during growth on the electron-rich substrate butyrate. Under chemotrophic conditions, we tested if nitrogen oxides can serve as an essential electron acceptor to generate energy via oxidative phosphorylation. As expected, each bacterium was only able to grow using the nitrogen oxides for which corresponding reductases were annotated in their genomes. However,  $\text{N}_2\text{O}$  utilization required supplementation with additional nitrogen oxides other than  $\text{N}_2\text{O}$ , including nitrogen oxides for which there was no predicted reductase and which did not support growth on their own. Our results indicate that at least some partial denitrifiers require nitrogen oxides that they cannot respire to reduce  $\text{N}_2\text{O}$ .

## RESULTS

### *R. palustris* CGA0092 has a partial denitrification pathway

*R. palustris* is one of the most-studied of the metabolically versatile PNSB (13), yet little is known about its ability to respire anaerobically. Unlike some other model, PNSB, CGA009, and its derivative CGA0092 (14) used herein cannot grow via respiration with dimethylsulfoxide (15–17). However, according to its genome sequence, it should be capable of partial denitrification, as it has putative enzymes for converting  $\text{NO}_2^-$  to  $\text{N}_2$  (10, 13) (Fig. 1B). Expanding on past analyses by others (10, 13), we used PSI-BLAST to verify that there are no genes with significant similarity to *nar*, *nap*, or *nas* nitrate reductase genes or to *nasB*, *nirB*, *nirD*, *nirA*, *nrf*, or eight-heme nitrite reductase genes (Table S1) (18).

When incubated anaerobically in darkness, PNSB typically use electron acceptors to establish a proton motive force and generate ATP. When incubated in light, PNSB generate ATP by photophosphorylation, but electron acceptors, such as  $\text{CO}_2$  or  $\text{NaHCO}_3$ , are required for growth on electron-rich compounds like butyrate to prevent an accumulation of reduced electron carriers, which halts metabolism; butyrate contains more electrons than can be incorporated into biomass, and so, the excess electrons must be deposited on an electron acceptor or released as  $\text{H}_2$  (19, 20). Given that *R. palustris* grows best in light, we first examined if it could use denitrification intermediates as electron acceptors during growth with butyrate.

In agreement with the apparent lack of  $\text{NO}_3^-$  reductase in the CGA0092 genome (Fig. 1B), phototrophic growth on butyrate was not supported when supplemented with a wide range of  $\text{NaNO}_3$  concentrations (Fig. 2A). However, growth was observed when CGA0092 was provided with 1 mM  $\text{NaNO}_2$  (Fig. 2A). We determined that this concentration was near the toxicity limit because it caused a lag in phototrophic growth on succinate, which does not require supplementation with an electron acceptor (Fig. 2B). We verified  $\text{NO}_2^-$  utilization using the colorimetric Griess assay. All of the  $\text{NO}_2^-$  removed could be accounted for in the accumulated  $\text{N}_2$  and  $\text{N}_2\text{O}$ , as measured by gas chromatography (Fig. 2C).  $\text{N}_2$  and  $\text{N}_2\text{O}$  levels were, in fact, higher than what could be explained by conversion of the supplied  $\text{NO}_2^-$ , although not significantly different from the expected 1:1 correspondence. If real, the excess nitrogen was likely due to contamination with atmospheric  $\text{N}_2$  during sampling and an inability to distinguish  $\text{N}_2\text{O}$  from  $\text{CO}_2$  produced by other metabolic reactions ( $\text{CO}_2$  and  $\text{N}_2\text{O}$  coeluted in our gas chromatography method).

Generation of  $\text{N}_2$  from  $\text{NO}_2^-$  indicated that the latter three reductases for denitrification are active in CGA0092. We did not directly address reduction of exogenously added

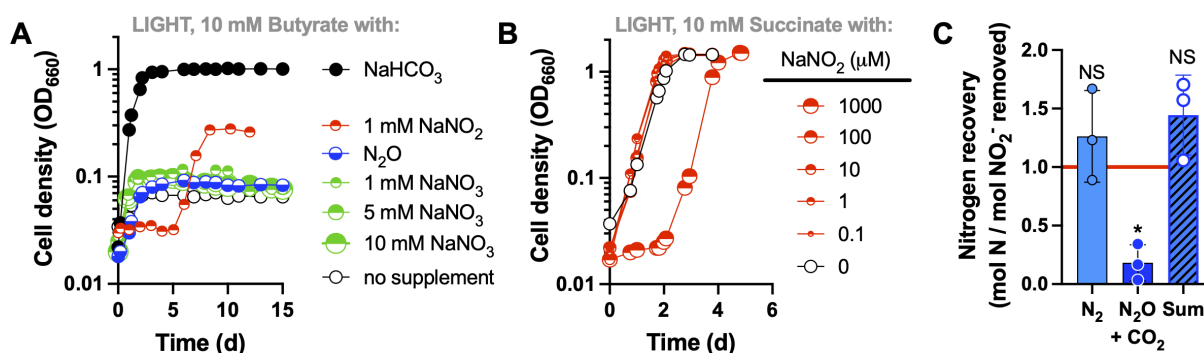


**FIG 2**  $\text{NaNO}_2$  supports phototrophic growth of CGA0092 on butyrate within toxicity limits. Cultures had a 100% Ar headspace unless  $\text{N}_2\text{O}$  is indicated (100%  $\text{N}_2\text{O}$ ). (A) Phototrophic growth with butyrate and various potential electron acceptors. Single representatives are shown. Similar trends were observed for three biological replicates except for conditions exploring different  $\text{NaNO}_3$  concentrations where only single representatives were used. (B) Phototrophic growth with succinate, a condition that readily supports growth without supplementation with an electron acceptor, with various concentrations of  $\text{NaNO}_2$  to identify the toxicity limit. (C) Proportion of  $\text{NO}_2^-$  recovered as  $\text{N}_2$  and  $\text{N}_2\text{O}$ . All of the supplied  $\text{NO}_2^-$  was removed.  $\text{N}_2\text{O}$  peak area includes a minor contribution of  $\text{CO}_2$  due to coelution during gas chromatography. Each point represents an independent biological replicate. Error bars = SD. \*, significantly different from 1 ( $P < 0.05$ ); NS, not significantly different from 1.0 ( $P > 0.05$ ), determined by a one-sample *t* and Wilcoxon test.

NO because it is highly toxic and would likely be impossible to add in amounts that would be practical to yield observable growth. We directly addressed N<sub>2</sub>O reduction by providing CGA0092 with a headspace of 100% N<sub>2</sub>O. However, no growth was observed within 15 days (Fig. 2A), suggesting that N<sub>2</sub>O alone cannot activate N<sub>2</sub>O reduction.

### Photoheterotrophic N<sub>2</sub>O reduction by CGA0092 requires NaNO<sub>2</sub> or NaNO<sub>3</sub>

In some bacteria, denitrification intermediates other than N<sub>2</sub>O enhance, or are required for, N<sub>2</sub>O reduction (1, 2, 21–23). For example, NO<sub>2</sub><sup>−</sup> can induce N<sub>2</sub>O reductase at the transcriptional level via the regulatory protein NnrR, although NO<sub>2</sub><sup>−</sup> might first need to be converted to NO (23). In *Bradyrhizobium diazoefficiens*, NO<sub>3</sub><sup>−</sup> induces N<sub>2</sub>O reductase via NasTS regulatory proteins and an anti-terminator mechanism that affects transcription of nos genes (24, 25). CGA0092 has an *nnrR* gene upstream of *nirK2* and, elsewhere in the genome, *nasTS* genes upstream of a gene cluster encoding a potential nitrite/sulfite reductase (RPA3710-11; Fig. 1B). We thus tested if NaNO<sub>2</sub> or NaNO<sub>3</sub> could enable growth with N<sub>2</sub>O. In agreement with our hypothesis, micromolar amounts of NaNO<sub>2</sub>, as low as 1 μM, stimulated growth with N<sub>2</sub>O, with final cell densities increasing in accordance with the amount of NaNO<sub>2</sub> added (Fig. 3A). NaNO<sub>2</sub> at 100 μM caused a 4-day lag in growth (Fig. 3A), suggesting that this level of NO<sub>2</sub><sup>−</sup> was slightly toxic under these conditions. Notably, the increase in final cell density afforded by high amounts of NaNO<sub>2</sub> depended on the presence of N<sub>2</sub>O, as growth with 100 μM NaNO<sub>2</sub> alone was much lower (Fig. 3A). This indicated that N<sub>2</sub>O was being used as the primary electron acceptor in the presence of NO<sub>2</sub><sup>−</sup>, despite that N<sub>2</sub>O could not serve as an electron acceptor when provided alone (Fig. 2A). We speculate that exhaustion of NO<sub>2</sub><sup>−</sup> eliminated the activation of N<sub>2</sub>O reduction, thereby eliminating the ability to use N<sub>2</sub>O as an electron acceptor; consequently, growth on butyrate with N<sub>2</sub>O lasts only as long as the pool of NaNO<sub>2</sub>.

Despite CGA0092 lacking NO<sub>3</sub><sup>−</sup> reductase, NaNO<sub>3</sub> was also sufficient to stimulate phototrophic growth on butyrate with N<sub>2</sub>O (Fig. 3B). Similar growth trends were observed between 1 μM to 10 mM NaNO<sub>3</sub>, indicating that NaNO<sub>3</sub> is relatively non-toxic and suggesting that NO<sub>3</sub><sup>−</sup> was not being reduced. Indeed, NO<sub>3</sub><sup>−</sup> levels were stable when we used 0.1 mM NaNO<sub>3</sub> to stimulate photoheterotrophic N<sub>2</sub>O reduction (Fig. 3C). The amount of N<sub>2</sub>O provided, all of which was ultimately removed, was linearly correlated with N<sub>2</sub> generated (Fig. 3C), although we again observed more N<sub>2</sub> generated than should be possible from the N<sub>2</sub>O provided, likely due to contamination with atmospheric N<sub>2</sub>. Culture growth and butyrate consumed were also linearly correlated with N<sub>2</sub>O supplied (and removed), further demonstrating the use of N<sub>2</sub>O as an electron acceptor (e.g., in place of NaHCO<sub>3</sub>; Fig. 2A) for phototrophic growth with butyrate.

To determine if the requirement of NaNO<sub>3</sub> or NaNO<sub>2</sub> for N<sub>2</sub>O reduction is manifested at the level of N<sub>2</sub>O reductase expression (the combination of transcription and translation), we created a reporter that fused the region upstream of *nosR*, which should contain both the native transcriptional promoter and ribosomal binding site, to a *lacZ* gene at the start codon and then integrated the reporter into the CGA0092 chromosome. We then grew the resulting reporter strain (CGA4070) under phototrophic conditions with acetate, a condition where an electron acceptor supplement is not required, and added NaCl (negative control), NaNO<sub>3</sub>, NaNO<sub>2</sub>, or N<sub>2</sub>O as a possible inducer of expression. In agreement with growth trends (Fig. 3), NaNO<sub>3</sub> and NaNO<sub>2</sub>, but not N<sub>2</sub>O, led to a significant, albeit low (1.6–2.4-fold), increase in LacZ activity over the NaCl control (Fig. 4). Thus, NaNO<sub>3</sub> and NaNO<sub>2</sub> are inducers of nos gene expression, although the relatively small effect suggests that there might be additional levels of regulatory control.

### N<sub>2</sub>O plus NaNO<sub>3</sub> can rescue photoheterotrophic growth of *R. palustris* Calvin cycle mutants

Under most photoheterotrophic growth conditions, the CO<sub>2</sub>-fixing Calvin cycle is essential to maintain electron balance, even on relatively oxidized substrates like succinate (19, 26, 27). To distinguish this essential electron balancing role from the Calvin cycle's better known role in carbon assimilation, alternative electron acceptors are a

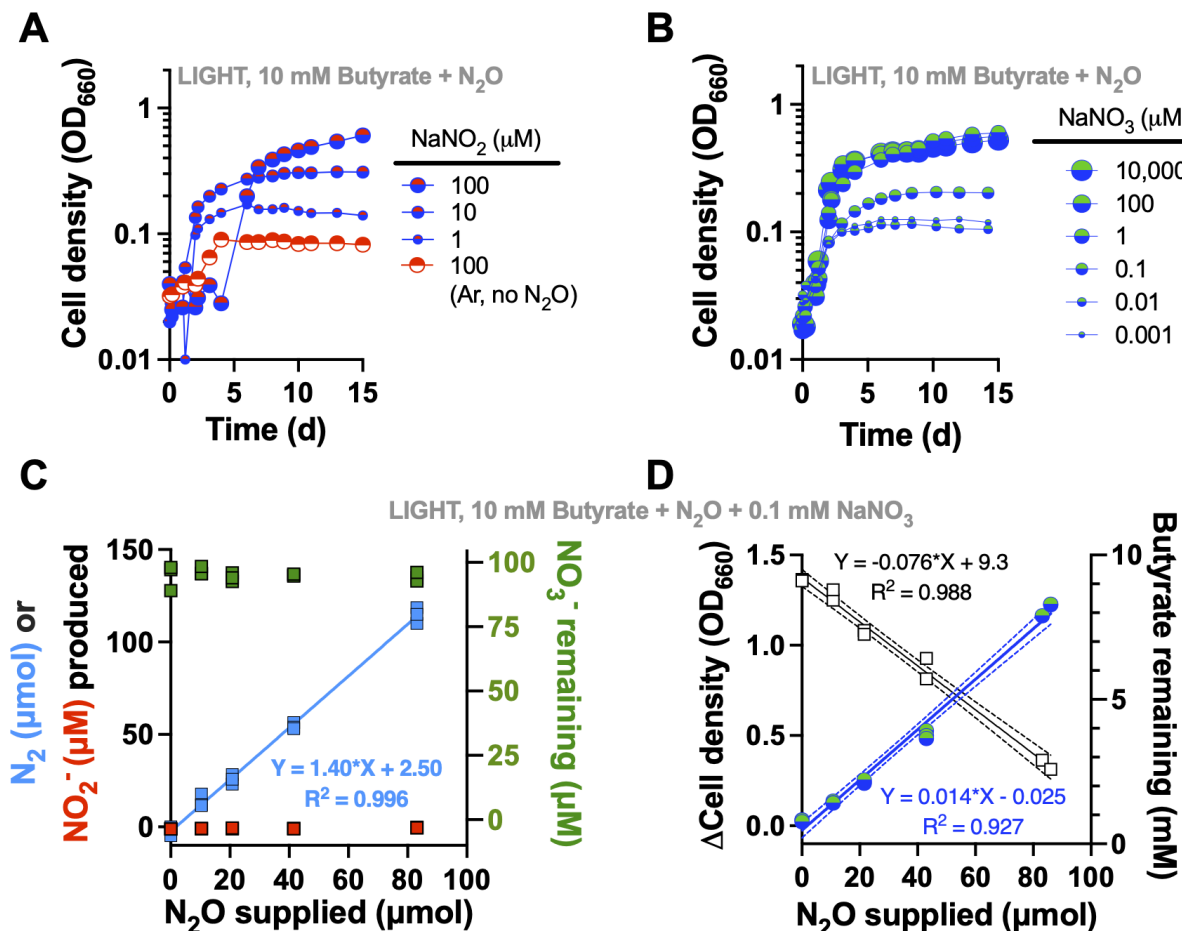


**FIG 3** NaNO<sub>2</sub> or NaNO<sub>3</sub> is required for phototrophic N<sub>2</sub>O utilization by CGA0092. (A) Phototrophic growth with butyrate ± N<sub>2</sub>O and different concentrations of NaNO<sub>2</sub>. The “Ar, no N<sub>2</sub>O” control had a 100% argon headspace. (B) Phototrophic growth with butyrate + N<sub>2</sub>O and different concentrations of NaNO<sub>3</sub>. Single representatives were surveyed. (C and D) Changes in N<sub>2</sub>, NO<sub>3</sub><sup>-</sup>, NO<sub>2</sub><sup>-</sup>, cell density, and butyrate in N<sub>2</sub>O-limited cultures. Measurements were taken at inoculation and when the maximum cell density was reached. Each point represents a single independent culture. Dashed lines = 95% CI. All N<sub>2</sub>O was removed by stationary phase. Linear regression for NO<sub>3</sub><sup>-</sup> (C) gave a slope that was not significantly different from zero ( $P = 0.57$ ).

useful tool because they permit growth of Calvin cycle mutants (28, 29). Thus far, the only method known to allow growth of *R. palustris* Calvin cycle mutants under conditions where the cycle is normally essential was via NifA\* mutations that result in constitutive nitrogenase activity (19, 26, 27). NifA\* mutants dispose of excess electrons as H<sub>2</sub>, an obligate product of the nitrogenase reaction. However, our results suggested that N<sub>2</sub>O could be used as an electron acceptor to grow *R. palustris* Calvin cycle mutants without additional genetic intervention. Indeed, N<sub>2</sub>O with NaNO<sub>3</sub> rescued an *R. palustris* Calvin cycle mutant (ΔCalvin) during phototrophic growth on succinate (Fig. 5). N<sub>2</sub>O reduction resulted in more immediate growth than a NifA\* mutation. However, growth eventually slowed, and the culture reached a lower final cell density than the ΔCalvin NifA\* mutant (Fig. 5). Gas chromatographic analysis of headspace samples confirmed that growth of cultures with N<sub>2</sub>O plus NaNO<sub>3</sub> was not due to spontaneous mutations that enabled H<sub>2</sub> production (i.e., no H<sub>2</sub> was detected; data not shown).

#### NaNO<sub>3</sub> does not improve *R. palustris* photoheterotrophic growth with NaNO<sub>2</sub>

We wondered if NaNO<sub>3</sub> might also improve growth with NO<sub>2</sub><sup>-</sup>, perhaps by stimulating NO<sub>2</sub><sup>-</sup> reductase activity. However, supplementation with NaNO<sub>3</sub> did not affect photoheterotrophic growth trends on butyrate with 1 mM NaNO<sub>2</sub>, even when NaNO<sub>3</sub> was also added to starter cultures as a possible “pre-inducing” condition (Fig. 6A). The same

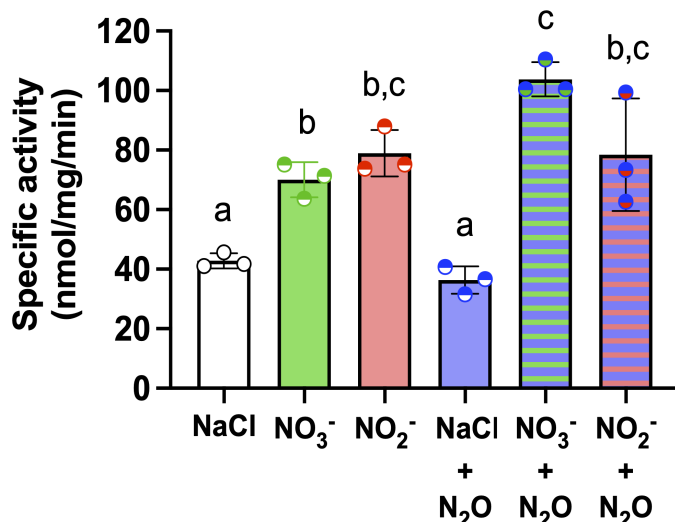


**FIG 4**  $\text{NaNO}_3$  and  $\text{NaNO}_2$ , but not  $\text{N}_2\text{O}$ , positively affect *nosR* expression.  $\beta$ -Galactosidase measurements were made in cell extracts of CGA4070, which harbors a chromosomally integrated *nosR* promoter-*lacZ* fusion. CGA4070 was grown phototrophically with 23 mM acetate and 0.1 mM NaCl,  $\text{NaNO}_3$ , or  $\text{NaNO}_2$ . Cultures received 4-mL  $\text{N}_2\text{O}$ , where indicated. Each point represents a single independent culture. All values were corrected for a background *o*-nitrophenol production rate of 8.7 nmol/mg/min as measured in cell extracts from CGA0092 grown under identical conditions with 0.1 mM NaCl or  $\text{NaNO}_3$ ; activity was not significantly different between conditions with NaCl or  $\text{NaNO}_3$ . Error bars = SD. Floating letters indicate significant differences between strains (one-way analysis of variance with Tukey post-test;  $P < 0.05$ ).

strategy also did not decrease the lag phase during phototrophic growth on succinate with 1 mM  $\text{NaNO}_2$  (Fig. 6B).

#### $\text{NaNO}_3$ is required for anaerobic respiration with $\text{N}_2\text{O}$ by CGA0092 in the dark

Without access to light, many PNSB can grow chemoheterotrophically via anaerobic respiration. We tested if  $\text{NaNO}_2$  or  $\text{N}_2\text{O}$  could support chemoheterotrophic growth by CGA0092 in the dark. Acetate and butyrate were chosen as two carbon sources that are metabolized via similar pathways but contain different amounts of electrons (19). Unlike phototrophic conditions (Fig. 2), supplementation with either 0.3 or 1 mM  $\text{NaNO}_2$  did not support observable growth in the dark with either acetate or butyrate within 15 days. In contrast,  $\text{N}_2\text{O}$  supported growth with either acetate or butyrate but only when  $\text{NaNO}_3$  was also provided (Fig. 7). Because growth was slower with acetate than with butyrate (doubling time  $\pm$  SD =  $88 \pm 2$  h vs  $51 \pm 3$ , respectively), we performed further analyses with butyrate. As during phototrophy (Fig. 3), chemotrophic  $\text{N}_2$  production, culture growth, and butyrate consumption were linearly correlated with the amount of  $\text{N}_2\text{O}$  provided (Fig. 7C and D). All or nearly all  $\text{N}_2\text{O}$  was removed, while  $\text{NO}_3^-$  levels remained stable, without  $\text{NO}_2^-$  production (Fig. 7C).

The chemotrophic growth rate and growth yield with butyrate were 24% and 17%, respectively, of those observed under phototrophic  $\text{N}_2\text{O}$ -reducing conditions (Table 1). However, the specific rate of  $\text{N}_2\text{O}$  reduction was 1.4-fold higher under chemotrophic conditions (Table 1), suggesting that the rate of  $\text{N}_2\text{O}$  reduction needed to support electron balance under phototrophic conditions is less than that possible when  $\text{N}_2\text{O}$  reduction is needed for energy transformation. In agreement with the lower growth yield, the  $\text{N}_2\text{O}$  product yield ( $\text{N}_2\text{O}$  removed per butyrate consumed) was 3.3-fold higher under chemotrophic conditions (Table 1), indicating that more electrons from butyrate were directed to energy transformation compared to biosynthesis during chemotrophic growth.

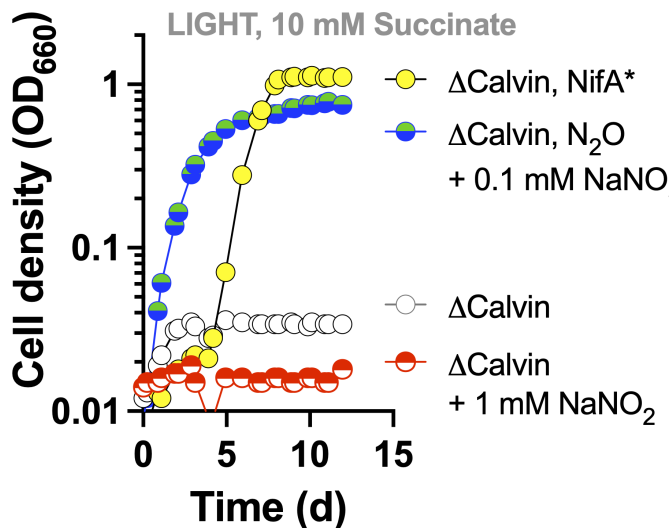


**FIG 5**  $\text{N}_2\text{O}$  plus  $\text{NaNO}_3$  supports phototrophic growth of an *R. palustris* Calvin cycle deletion mutant. Cultures had a 100% Ar headspace unless  $\text{N}_2\text{O}$  is indicated (100%  $\text{N}_2\text{O}$ ). Single representatives are shown. Similar trends were observed for three biological replicates.  $\Delta\text{Calvin}$  is strain CGA4008;  $\Delta\text{Calvin NifA}^*$  is strain CGA4011.

#### $\text{NaNO}_2$ is required for phototrophic $\text{N}_2\text{O}$ reduction by *R. capsulatus* SB1003

We wondered if the requirement for non-catalyzable denitrification intermediates for  $\text{N}_2\text{O}$  utilization was specific to *R. palustris* or if the same was true for other partial denitrifiers. To examine this possibility, we turned to *R. capsulatus* SB1003, which stood out as an easily cultivatable and phylogenetically distant PNSB that is annotated to only have  $\text{N}_2\text{O}$  reductase (10) (Fig. 8A). Using PSI-BLAST, we built upon past analyses (10) and confirmed that SB1003 does not have genes with significant similarity to known assimilatory and dissimilatory  $\text{NO}_3^-$  and  $\text{NO}_2^-$  reductase genes (Table S1). As predicted, phototrophic growth of SB1003 on butyrate was not supported by  $\text{NaNO}_3$  or  $\text{NaNO}_2$  (Fig. 8B), although our ability to assess the latter was limited by the sensitivity of SB1003 to  $\text{NaNO}_2$  concentrations  $>0.5$  mM (Fig. 8C). Similar to what was observed for *R. palustris*,  $\text{N}_2\text{O}$  alone did not support phototrophic growth of SB1003 (Fig. 8B). However, supplementation with 0.1 mM  $\text{NaNO}_2$  but not  $\text{NaNO}_3$  led to phototrophic growth on butyrate with  $\text{N}_2\text{O}$  (Fig. 8B). Also,  $\text{N}_2$  production, growth, and butyrate production were

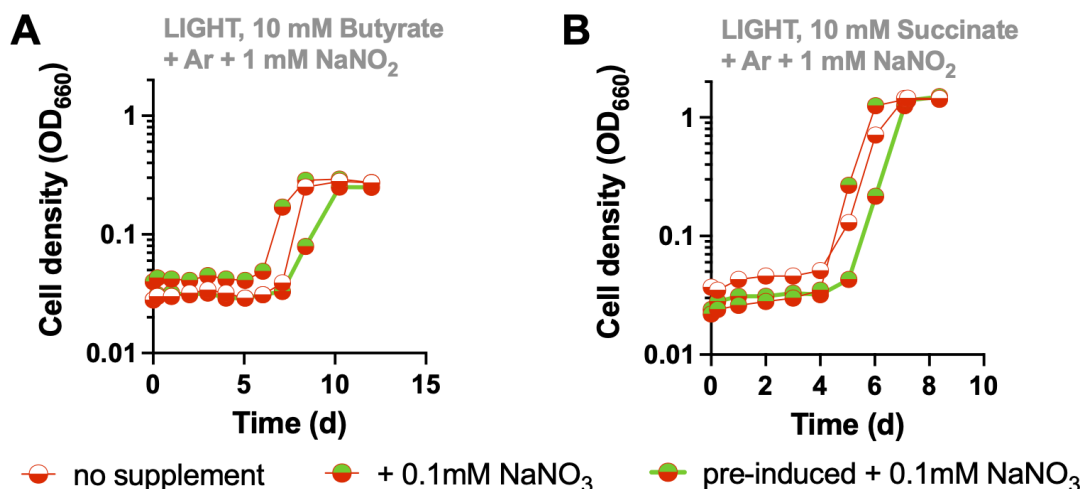


**FIG 6**  $\text{NaNO}_3$  does not improve growth trends when  $\text{NaNO}_2$  is present as an essential electron sink (A) or as a toxic compound (B). Single representatives are shown. Similar trends were observed for three biological replicates.

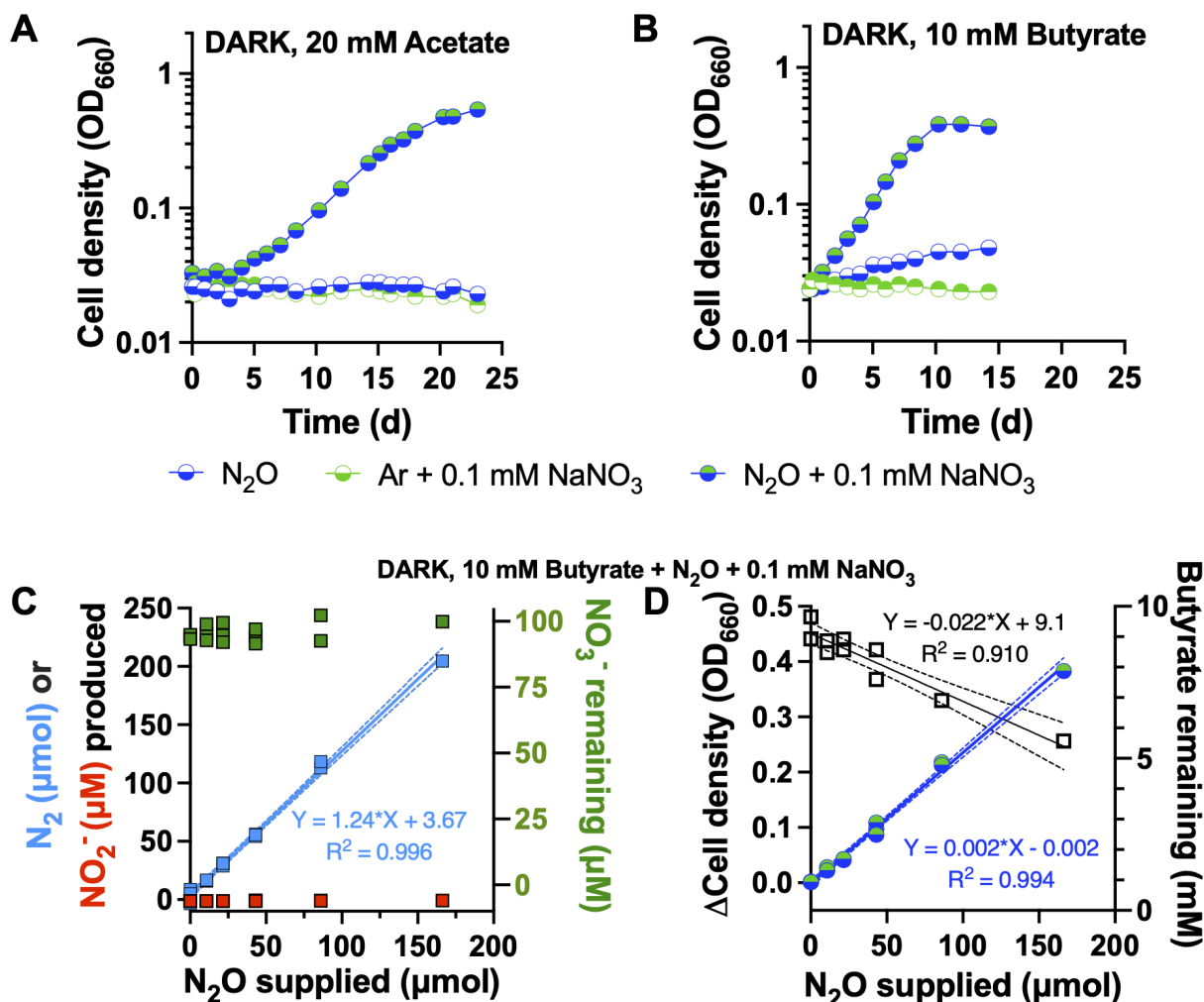


FIG 7 NaNO<sub>3</sub> is required for N<sub>2</sub>O respiration by CGA0092 in the dark with acetate (A) or butyrate (B). Single representatives are shown. Similar trends were observed for three biological replicates. Cultures had a 100% Ar headspace or 100% N<sub>2</sub>O headspace as indicated. (C and D) Changes in N<sub>2</sub>, NO<sub>3</sub><sup>-</sup>, cell density, and butyrate in N<sub>2</sub>O-limited cultures. Measurements were taken at inoculation and when the maximum cell density was reached. Each point represents a single independent culture. Dashed lines = 95% CI. Most or all N<sub>2</sub>O was removed by stationary phase. Linear regression for NO<sub>3</sub><sup>-</sup> (C) gave a slope that was not significantly different from zero ( $P = 0.11$ ).

linearly correlated with the amount of N<sub>2</sub>O provided (Fig. 8D and E), with all or nearly all N<sub>2</sub>O removed. However, unlike with *R. palustris*, levels of the stimulating compound, in this case, NO<sub>2</sub><sup>-</sup>, were not stable. NO<sub>2</sub><sup>-</sup> concentration declined with a roughly linear correlation to the amount of N<sub>2</sub>O provided (Fig. 8D). NO<sub>3</sub><sup>-</sup> concentrations remained close to zero (Fig. 8D), suggesting that NO<sub>2</sub><sup>-</sup> was reduced, rather than oxidized. The specific rate of N<sub>2</sub>O reduction was 300 times higher than that of NO<sub>2</sub><sup>-</sup> reduction (Table 1). This disparity suggests that NO<sub>2</sub><sup>-</sup> removal was likely due to a promiscuous enzyme activity or a growth-correlated abiotic factor rather than due to an unannotated bona fide NO<sub>2</sub><sup>-</sup> reductase.

#### NaNO<sub>2</sub> is required for anaerobic respiration with N<sub>2</sub>O by SB1003 in the dark

SB1003 could also respire N<sub>2</sub>O in the dark with butyrate but again only when NaNO<sub>2</sub> was also present (Fig. 9A). Most or all N<sub>2</sub>O was converted to N<sub>2</sub> when limiting amounts of N<sub>2</sub>O was provided in the presence of 0.1 mM NaNO<sub>2</sub> (Fig. 9B). N<sub>2</sub>O supplied also showed linear correlation with culture growth and butyrate consumption (Fig. 9C). Although only a small amount, some NO<sub>2</sub><sup>-</sup> was likely removed during N<sub>2</sub>O reduction because

TABLE 1 Growth and metabolic parameters from N<sub>2</sub>O-reducing conditions with butyrate<sup>a</sup>

Strain, growth condition	Sp growth rate (d <sup>-1</sup> )	Doubling time (d) <sup>b</sup>	Sp N <sub>2</sub> O reduction rate (fmol/CFU/d) <sup>c</sup>	Sp NO <sub>2</sub> <sup>-</sup> reduction rate (fmol/CFU/d) <sup>c</sup>	Growth yield (CFU/pmol N <sub>2</sub> O) <sup>d</sup>	Growth yield (CFU/pmol butyrate) <sup>d</sup>	N <sub>2</sub> O product yield (mol/mol butyrate) <sup>d</sup>
CGA0092, light	1.36 ± 0.09	0.51 ± 0.04	1,877 ± 182	ND	70 ± 5	90 ± 10	1.3 ± 0.1
CGA0092, dark	0.32 ± 0.02	2.20 ± 0.16	2,645 ± 221	ND	12 ± 0	50 ± 10	4.3 ± 0.8
SB1003, light	1.32 ± 0.18	0.53 ± 0.07	1,503 ± 229	5 ± 3	87 ± 6	105 ± 5	1.6 ± 0.3
SB1003, dark	0.79 ± 0.16	0.87 ± 0.02	6,332 ± 1,348	5 ± 4	13 ± 0	75 ± 10	5.9 ± 0.8

<sup>a</sup>Values show averages ± 95% CI. CFU, colony-forming units.

<sup>b</sup>Doubling time = ln2/growth rate.

<sup>c</sup>Specific (Sp) reduction rates were determined from N<sub>2</sub>O-limited cultures as described in the methods.

<sup>d</sup>Product yields were determined from N<sub>2</sub>O-limited cultures by linear regression. N<sub>2</sub>O product yield is the amount of N<sub>2</sub>O removed per butyrate consumed.

the linear correlation of NO<sub>2</sub><sup>-</sup> levels with N<sub>2</sub>O supplied was negative and significantly different from zero (Fig. 9B). The specific NO<sub>2</sub><sup>-</sup> reduction rate was three orders of

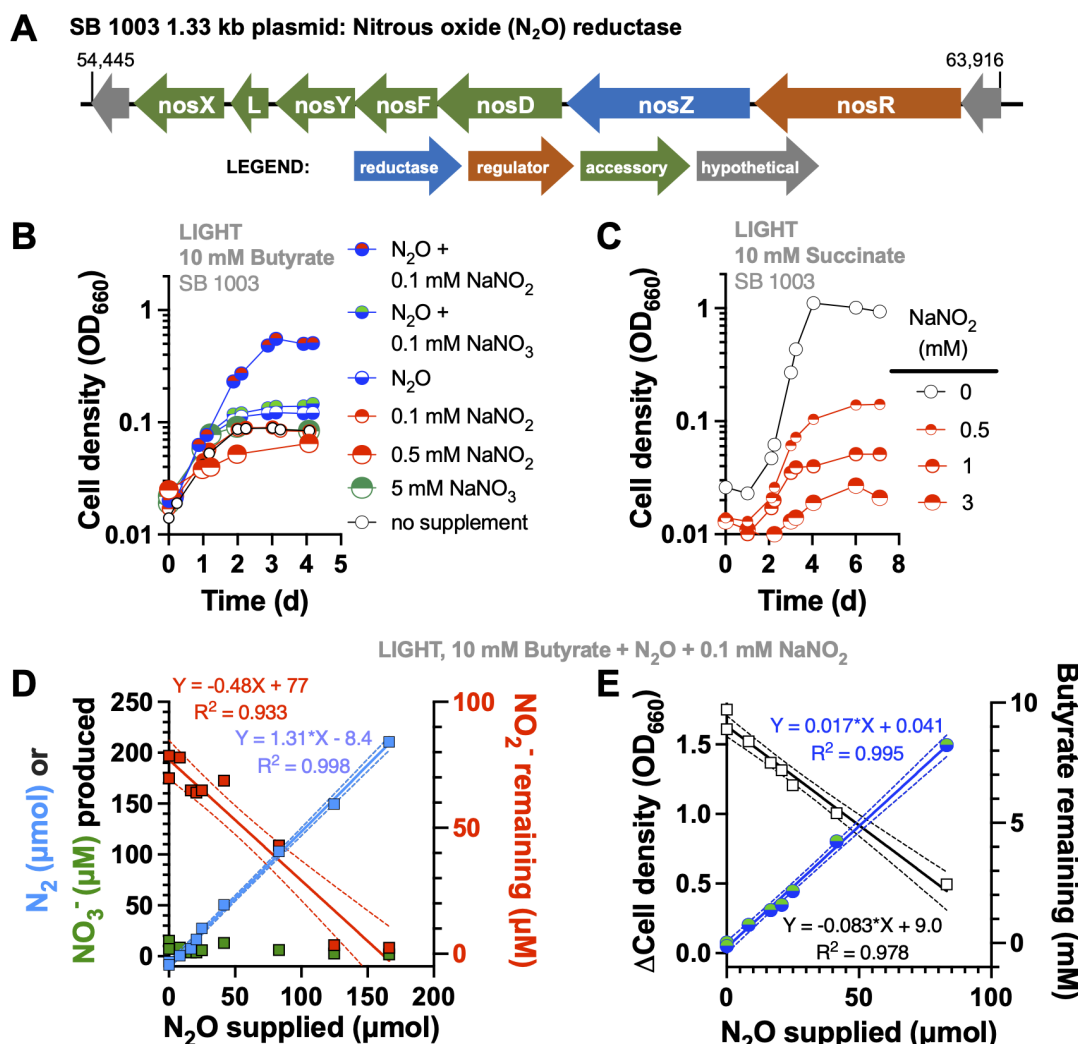


FIG 8 NaNO<sub>2</sub> is required for phototrophic N<sub>2</sub>O reduction by *R. capsulatus* SB1003. (A) Plasmid location of predicted N<sub>2</sub>O reductase genes (nos). Numbers indicate nucleotide positions. (B) Phototrophic growth with butyrate and various denitrification intermediates. Single representatives are shown. Similar trends were observed for three biological replicates. Cultures had a 100% Ar headspace unless N<sub>2</sub>O is indicated (100% N<sub>2</sub>O). (C) Phototrophic growth with succinate and various NaNO<sub>2</sub> concentrations to determine the toxicity limit. Single representatives were surveyed. (D and E) Changes in N<sub>2</sub>, NO<sub>3</sub><sup>-</sup>, cell density, and butyrate in N<sub>2</sub>O-limited cultures. Measurements were taken at inoculation and when the maximum cell density was reached. Each point represents a single independent culture. Dashed lines = 95% CI. Samples were diluted in cuvettes where necessary to ensure linear correlation between OD and cell density. Most or all N<sub>2</sub>O was removed by stationary phase. Linear regression for NO<sub>2</sub><sup>-</sup> (D) gave a slope that was significantly different from zero ( $P = 0.0002$ ).

magnitude slower than the specific  $\text{N}_2\text{O}$  reduction rate (Table 1), again suggesting that the activity was not associated with a canonical denitrification reaction. Similar to *R. palustris*, the SB1003 chemotrophic growth rate and growth yield were lower than those in phototrophic conditions, and more electrons in butyrate were diverted to  $\text{N}_2\text{O}$  reduction compared to biosynthesis (Table 1). However, SB1003 appears to be capable of a 2.4-fold higher specific  $\text{N}_2\text{O}$  reduction rate, which likely explains the proportionately higher chemotrophic growth rate compared to *R. palustris* CGA0092 (Table 1).

## DISCUSSION

Here, we verified that *R. palustris* CGA0092 and *R. capsulatus* SB1003 are partial denitrifiers, with each being capable of respiring the nitric oxides predicted from their genome annotations (both organisms have been sequenced to closed genomes). We observed that these bacteria can only reduce  $\text{N}_2\text{O}$  when supplied with other denitrification intermediates. Most importantly, nitrogen oxides required for  $\text{N}_2\text{O}$  reduction include those outside of each organism's partial denitrification repertoire, that is,  $\text{NO}_3^-$  in the case of CGA0092 and  $\text{NO}_2^-$  in the case of SB1003.

### $\text{NO}_3^-$ as a non-catalyzable inducer of *nos* gene expression

Using a *lacZ* reporter under control of an *R. palustris* *nosR* promoter, we found that  $\text{N}_2\text{O}$  reduction is induced by  $\text{NO}_3^-$  and  $\text{NO}_2^-$ , at least in part, at the level of gene expression (our construct likely captures transcriptional and translational regulatory features). The level of induction was low compared to the 10-fold increase seen with a *B. diazoeficiens* *nosZ*–*lacZ* reporter (24, 30). One possible explanation for the discrepancy is our use of a *nosR* promoter–*lacZ* fusion. NosR is a required regulatory protein for nitrous oxide reductase activity (31, 32) that is typically encoded with little to no intergenic region between *nosR* and *nosZ* (Fig. 1). While the *nosR* promoter drives *nosZ* expression in some bacteria (23), in other bacteria, *nosZ* expression can occur from separate and sometimes multiple transcriptional start sites (25, 33). Substantial work beyond the current study will be necessary to decipher the transcriptional and post-transcriptional regulatory mechanisms governing *R. palustris* *nos* genes. However, our findings clearly indicate that  $\text{NO}_3^-$  or  $\text{NO}_2^-$  is required for  $\text{N}_2\text{O}$  reduction by *R. palustris* CGA0092 and that each of them plays a role as an inducer of *nos* gene expression.

### Modification of $\text{NO}_2^-$ and $\text{NO}_3^-$ ?

A caveat to the observed activation of  $\text{N}_2\text{O}$  reduction activity by  $\text{NO}_2^-$  and  $\text{NO}_3^-$  is that some promiscuous biotic or abiotic transformation could be necessary to generate the

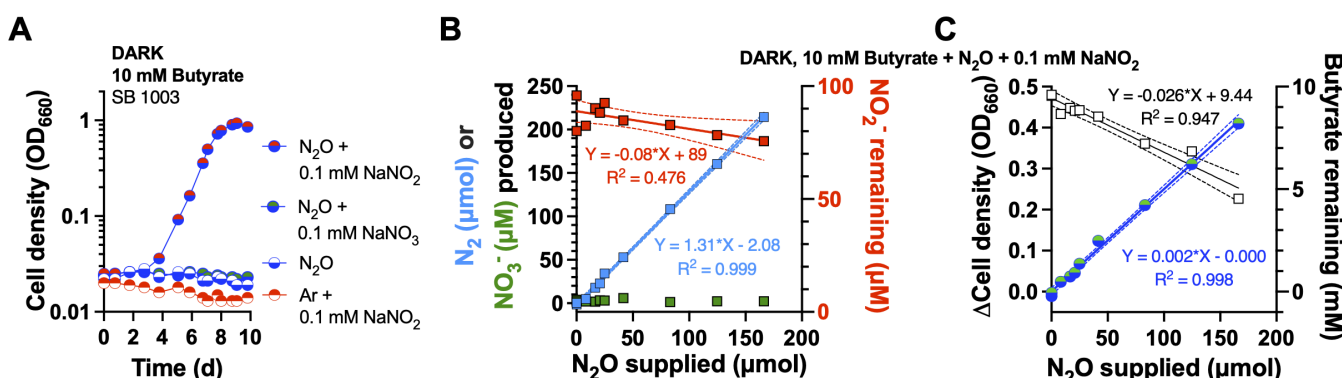


**FIG 9**  $\text{NaNO}_2$  is required for  $\text{N}_2\text{O}$  respiration by SB1003 in the dark. (A) Chemotrophic growth of SB1003 on butyrate with  $\text{N}_2\text{O}$  as an electron acceptor. Single representatives are shown. Similar trends were observed for three biological replicates. Cultures had a 100% Ar headspace unless  $\text{N}_2\text{O}$  is indicated (100%  $\text{N}_2\text{O}$ ). (B and C) Changes in  $\text{N}_2$ ,  $\text{NO}_3^-$ , cell density, and butyrate in  $\text{N}_2\text{O}$ -limited cultures. Measurements were taken at inoculation and when the maximum cell density was reached. Each point represents a single independent culture. Dashed lines = 95% CI. Most or all  $\text{N}_2\text{O}$  was removed by stationary phase. Linear regression for  $\text{NO}_3^-$  (B) gave a slope that was significantly different from zero ( $P = 0.0097$ ).

inducing/activating molecule. We hypothesize that a promiscuous enzyme activity led to the slow  $\text{NO}_2^-$  removal in SB1003 cultures (Fig. 8 and 9). One possible candidate is sulfite reductase (CysIJ; RCAP\_rcc01594 and 03007), which bears homology to assimilatory nitrite reductase. In *E. coli*, CysIJ can convert  $\text{NO}_2^-$  to  $\text{NH}_4^+$  1.7 times faster than sulfite reduction but with a 200-fold lower affinity for  $\text{NO}_2^-$  compared to sulfite ( $k_m = 0.8 \text{ mM } \text{NO}_2^-$ , 8 times above the concentration used in our SB1003 experiments) (34). If CysIJ was responsible for  $\text{NO}_2^-$  removal, then  $\text{NO}_2^-$  was likely the molecule activating  $\text{N}_2\text{O}$  reduction because CysIJ would convert  $\text{NO}_2^-$  to  $\text{NH}_4^+$ , which was already present at millimolar concentrations in the growth medium. However, there could be another enzymatic or spontaneous activity reducing  $\text{NO}_2^-$  to NO as a separate inducing molecule. For CGA0092, levels of  $\text{N}_2\text{O}$  reductase-inducing  $\text{NO}_3^-$  were stable. However, it is still possible that some of the 100  $\mu\text{M } \text{NO}_3^-$  was converted below our detection limit to  $\text{NO}_2^-$  and/or NO. These molecules can induce  $\text{N}_2\text{O}$  reductase in other organisms like *P. aeruginosa*, although they are typically applied at the micromolar or millimolar levels (23).

### Possible regulators of $\text{N}_2\text{O}$ reduction

Our work calls for future investigation into the regulatory mechanisms controlling  $\text{N}_2\text{O}$  reduction in CGA0092 and SB1003. However, we can speculate on the regulatory proteins involved based on genome annotations. In considering  $\text{NO}_3^-$  as an inducing molecule in CGA0092, NasTS stands out as a candidate. In *B. diazocephiens*, NasTS controls the transcriptional activation of *nos* genes (24, 25). CGA0092 has genes with significant sequence identity to *B. diazocephiens* NasTS (77% and 66% amino acid identity, respectively; Fig. 1B). NnrR (Fig. 1B) could also be involved in regulating  $\text{N}_2\text{O}$  reductase, although more likely in response to NO (1, 23, 35–37).

$\text{NO}_2^-$  could also activate  $\text{N}_2\text{O}$  reduction in SB1003 via an NnrR-like regulator. SB1003 has several CRP/Fnr family transcriptional regulator genes encoded in its chromosome with >25% amino acid identity to denitrification regulators like *P. denitrificans* FnrP (RCAP\_rcc02493; 74% identity) and *Pseudomonas aeruginosa* Dnr/NnrR (e.g., RCAP\_rcc00107; 36% identity). One or more of these regulators could be involved in regulating  $\text{N}_2\text{O}$  reductase, although more likely in response to NO generated biotically or abiotically from  $\text{NO}_2^-$  (23).

### Denitrification inventories should consider both reductases and regulators

Denitrification gene inventories are notoriously inconsistent with organismal phylogeny; it is common for one species to carry more or less denitrification genes than a close relative (8–10, 12, 38, 39). This inconsistency is also true for strains of *R. palustris* and *R. capsulatus* (20, 40–43). In some cases, horizontal gene transfer (HGT) could explain the phylogenetic discrepancies. The location of the *nos* operon on a plasmid in SB1003 is a straightforward example of HGT (Fig. 8A). However, HGT cannot explain many of the chromosomal phylogenetic discrepancies. Phylogenetic analyses have suggested the involvement of other factors like gene duplication and divergence, lineage sorting (38), and gene loss (12). Gene loss could be advantageous in communities where there are redundant denitrification functions. As proposed in the Black Queen Hypothesis (44), gene loss can occur when the cost of producing a public good exceeds the benefit of obtaining it from a neighbor. In this case, the cost of a full denitrification pathway could drive loss of denitrification genes if sufficient energy can be obtained by using a denitrification intermediate released by a neighbor (12). Benefits of partial denitrification pathways have been demonstrated in a synthetic community, although the benefits stemmed more from  $\text{NO}_2^-$  detoxification than energy savings (45).

Inventories of denitrification regulators have not received the same level of phylogenetic scrutiny as the reductases. Such analyses would be complicated by the fact that phylogenetically similar regulators can regulate different genes (46). However, regulator inventories are likely an important determinant of reductase inventories because improper regulation could influence maintenance or loss of a reductase gene. Regulator

inventories also raise questions about the evolutionary histories of denitrification genes. For example, if *NasTS* is required for expression of the *nos* operon in *R. palustris* CGA0092, were both regulator and reductase genes serendipitously acquired at the same time as separate DNA molecules by HGT or were they acquired together as a single DNA molecule and then physically separated through genome rearrangements (Fig. 1B)? Alternatively, perhaps, the common ancestor to CGA0092 and *B. diazoeficiens* USDA110 was capable of complete denitrification, and CGA0092 lost nitrate reductase genes but retained the native regulatory network that was responsive to  $\text{NO}_3^-$ . Both genera clade together within the Nitrobacteraceae family, but the CGA0092 genome is 3.4 Mb smaller than that of USDA110, and in each case, the *nasTS* and the *nos* genes are separated by large stretches of chromosome (~2 Mb in CGA0092 and ~5 Mb in USDA110). Regulator inventory might also support a community role for partial denitrifiers. The regulation of  $\text{N}_2\text{O}$  reductase by  $\text{NO}_3^-$  and  $\text{NO}_2^-$  in this study could suggest that CGA0092 and SB1003 are primed to sense signals by denitrifying partners.

Our findings suggest that within communities of partial denitrifiers, nitric oxides are not only cross-fed metabolites but also important regulatory molecules. The requirement of these molecules for  $\text{N}_2\text{O}$  reduction is an important consideration in efforts to mitigate greenhouse gas emissions from agricultural soils, which is the largest source of  $\text{N}_2\text{O}$  emissions (6). Given that agricultural soils are fertilized with  $\text{NO}_3^-$ , we do not anticipate a shortage of  $\text{NO}_3^-$  in those environments. However, our findings expose a potential pitfall in overlooking the capacity of *nosZ*-harboring bacteria to reduce  $\text{N}_2\text{O}$ , if unanticipated inducing molecules are omitted from lab cultures.

## MATERIALS AND METHODS

### Strains

*R. palustris* CGA0092 is a chloramphenicol-resistant type strain derived from CGA001 and differs from CGA009 by a single-nucleotide polymorphism (13, 14). The Calvin cycle mutant  $\Delta cbbLSMP::km^R$  ( $\Delta$ Calvin, CGA4008) was constructed by deleting *cbbLS*, encoding ribulose-1,5-bisphosphate carboxylase (Rubisco) form I, in a previously described mutant lacking Rubisco form II [ $\Delta cbbM$ ; CGA668 (26)] via introduction of the suicide vector pJQ $\Delta cbbLS$  (47) by conjugation with *E. coli* S17 as described (47, 48). The gene encoding phosphoribulokinase, *cbbP*, was then deleted in the resulting strain ( $\Delta cbbLSM$ ; CGA4006) by introducing the suicide vector pJQ $\Delta cbbP::km^r$  (47), as above, to generate the  $\Delta cbbLSMP::km^R$  strain, CGA4008. The elimination of three enzymes unique to the Calvin cycle greatly decreases the odds of enriching for suppressor mutations. All strain genotypes were verified by PCR and Sanger sequencing. CGA4011 is a NifA\* derivative of CGA4008 that has constitutive nitrogenase activity/ $\text{H}_2$  production (47). *R. capsulatus* SB1003 was provided courtesy of Carl Bauer (Indiana University).

CGA4070 was derived from CGA0092 for assaying *nosR* promoter activity using a *lacZ* reporter chromosomally integrated upstream of the *nos* gene cluster, a similar strategy as that used in *B. diazoeficiens* (24, 49). Briefly, a 398-nt region upstream of the *nosR* start codon was synthesized in front of *lacZ* and incorporated into pTwist Kan High Copy plasmid by Twist Bioscience (<https://www.twistbioscience.com/>) to create pTwist\_PNos-LacZ. CGA0092 was transformed with pTwist\_PNos-LacZ by electroporation and plated on photosynthetic medium (PM) agar with 10 mM succinate and 100  $\mu\text{g}/\text{mL}$  kanamycin. Colonies were screened for integration by both PCR and by the appearance of blue color when patched to identical agar that also contained 5-bromo-4-chloro-3-indolyl- $\beta$ -D-galactoside.

### Growth conditions

Strains were routinely cultivated in 10-mL PM in 27-mL anaerobic test tubes. PM is based on described media compositions (50, 51) and contains (final concentrations) the following: 12.5 mM  $\text{Na}_2\text{HPO}_4$ , 12.5 mM  $\text{KH}_2\text{PO}_4$ , 7.5 mM  $(\text{NH}_4)_2\text{SO}_4$ , 0.1 mM  $\text{Na}_2\text{S}_2\text{O}_3$ ,

15  $\mu$ M p-aminobenzoic acid, and 1 mL/L concentrated base (51). Concentrated base contains the following: 20 g/L nitriloacetic acid, 28.9 g/L MgSO<sub>4</sub>, 6.67 g/L CaCl<sub>2</sub>·2H<sub>2</sub>O, 0.019 g/L (NH<sub>4</sub>)<sub>6</sub>Mo<sub>7</sub>O<sub>24</sub>·4H<sub>2</sub>O, 0.198 g/L FeSO<sub>4</sub>·7H<sub>2</sub>O, and 100 mL/L Metals 44 (52). Metals 44 contains the following: 2.5 g/L ethylenediaminetetraacetic acid, 10.95 g/L ZnSO<sub>4</sub>·7H<sub>2</sub>O, 5 g/L FeSO<sub>4</sub>·7H<sub>2</sub>O, 1.54 g/L MnSO<sub>4</sub>·H<sub>2</sub>O, 0.392 g/L CuSO<sub>4</sub>·5H<sub>2</sub>O, 0.25 g/L Co(NO<sub>3</sub>)<sub>2</sub>·6H<sub>2</sub>O, and 0.177 g/L Na<sub>2</sub>B<sub>4</sub>O<sub>7</sub>·10H<sub>2</sub>O. PM was made anaerobic by bubbling tubes with 100% Ar and then sealing with rubber stoppers and aluminum crimps prior to autoclaving. After autoclaving, tubes were supplemented with either 20 mM sodium acetate, 10 mM sodium butyrate, or 10 mM disodium succinate from 100 $\times$  anaerobic stock solutions. Where indicated, cultures were additionally supplemented with 20 mM NaHCO<sub>3</sub>. SB1003 cultures were also supplemented with 0.1  $\mu$ g/mL nicotinic acid, 0.2  $\mu$ g/mL riboflavin, and 1.3  $\mu$ g/mL thiamine-HCl. NaNO<sub>2</sub> or NaNO<sub>3</sub> was added from anaerobic stock solutions to the final concentrations indicated in the text. For conditions with N<sub>2</sub>O, tubes were flushed with 100% N<sub>2</sub>O through a 0.45- $\mu$ m syringe filter and needle after all liquid supplements were added. A second needle was used for off-gassing. For N<sub>2</sub>O-limited cultures, the indicated volume of filtered gas was added via syringe. Cultures were inoculated with a 1% inoculum from starter cultures grown phototrophically in anaerobic PM with succinate, except for the experiment testing Calvin cycle mutants (Fig. 3C) in which all starter cultures were grown aerobically in 3-mL PM with succinate in the dark. These aerobic conditions were used to accommodate the *ΔcbbLSMP::km<sup>R</sup>* mutant (CGA4008) that requires an electron sink to grow.

### Analytical procedures

Culture growth was monitored via optical density at 660 nm (OD<sub>660</sub>) using a Genesys 20 spectrophotometer (Thermo-Fisher, Waltham, MA, USA) directly in culture tubes without sampling. For N<sub>2</sub>O-limited cultures, samples were diluted in cuvettes where specified. Specific growth rates were calculated using OD<sub>660</sub> values between 0.1 and 1.0 where cell density and OD are linearly correlated. N<sub>2</sub>, N<sub>2</sub>O, and H<sub>2</sub> were sampled from culture headspace using a gas-tight syringe and analyzed using a Shimadzu GC-2014 gas chromatograph (GC) equipped with a thermal conductivity detector. GC conditions for H<sub>2</sub> were described previously (53). GC conditions for N<sub>2</sub> and N<sub>2</sub>O used He as a carrier gas at 20 mL/min, a 80/100 Porapak N column (6'  $\times$  1/8"  $\times$  2.1 mm; Supelco) at 170°C, an inlet temperature of 120°C, and a detector temperature of 155°C with a current of 150 mA. Gas standards were prepared by injecting specific volumes of pure gasses at 1 atm (41.6 mM based on the ideal gas law and a temperature of 293 K) into a stopper-sealed serum vial of known volume, containing with a few glass beads to aid in mixing. Gas standards were mixed by shaking, sampled with a gas-tight syringe, and then injected at 1 atm by releasing pressure prior to injection. Pressure was not released prior to injection for culture headspace samples. Syringes were flushed with He prior to each standard or sample injection to minimize contamination with atmospheric N<sub>2</sub>. NO<sub>3</sub><sup>-</sup> and NO<sub>2</sub><sup>-</sup> were measured using a colorimetric Griess assay kit according to the manufacturer's instructions (Cayman Chemical). Conversion of NO<sub>3</sub><sup>-</sup> to NO<sub>2</sub><sup>-</sup> was accomplished via NO<sub>3</sub><sup>-</sup> reductase provided with the kit. N<sub>2</sub>, N<sub>2</sub>O, NO<sub>3</sub><sup>-</sup>, and NO<sub>2</sub><sup>-</sup> were measured at the time of inoculation and at stationary phase. Where applicable, CFUs were determined using a conversion factor of 1 OD<sub>660</sub> = 5  $\times$  10<sup>8</sup> CFU/mL (54). Specific reduction rates were determined by multiplying the growth rate by the slope of a linear regression of product vs cell density (55, 56) from N<sub>2</sub>O-limited cultures.

### $\beta$ -Galactosidase reporter assays

*R. palustris* strains were grown to mid-late exponential phase (0.4–1.1 OD<sub>660</sub>) with 23 mM sodium acetate and 0.1 mM NaCl, NaNO<sub>3</sub>, or NaNO<sub>2</sub>, with or without 4-mL N<sub>2</sub>O. Cultures were then chilled on ice, and all subsequent processing was carried out between 0°C–4°C. Cells were harvested by centrifugation, supernatants were discarded, and cells were resuspended in 0.5-mL Z-buffer. Cells were lysed by five 20-s rounds of bead beating at maximum speed using a FastPrep-24 benchtop homogenizer (MP Biomedical),

with 5 min on ice between rounds. Cell debris was pelleted by centrifugation, and supernatant protein was quantified using Bio-Rad's Bradford assay kit. Cell lysate (50- $\mu$ L supernatant) was mixed with 100- $\mu$ L Z-buffer in wells of a 96-well plate. Reactions were started with the addition of 30  $\mu$ L of 4 mg/mL ortho-nitrophenyl- $\beta$ -galactoside. Formation of o-nitrophenol was monitored at 420 nm over time at 30°C using a BioTek Synergy plate reader. Specific activity was determined by linear regression of the initial velocity and normalized for protein concentration.

## Bioinformatics

PSI-BLAST used default parameters except for 500 targets, an expect threshold of 10, a word size of 3, and a PSI-BLAST threshold of 0.005 using the refseq\_protein database for bacteria. At least five iterations were run or until no further sequences were found. Accession numbers for the query sequences are in Table S1.

## Statistical analyses

GraphPad Prism v10 was used for all statistical analyses.

## ACKNOWLEDGMENTS

This work was supported in part by a National Science Foundation CAREER award (MCB-1749489); the Division of Chemical Sciences, Geosciences, and Biosciences, Office of Basic Energy Sciences, U.S. Department of Energy (DOE), through grant DE-FG02-05ER15707; the Office of Science (BER), U.S. DOE, through grant DE-FG02-07ER64482; and the Indiana University College of Arts and Sciences.

We are grateful to Doug Rusch, Julia van Kessel, Cristina Landeta, Nick Haas, José Heerdink-Santos, Jillian Lewis, William Rockliff, and Anika Hays for advice, reagents, and media preparation. We are also grateful to the anonymous reviewers for constructive feedback.

## AUTHOR AFFILIATIONS

<sup>1</sup>Department of Biology, Indiana University, Bloomington, Indiana, USA

<sup>2</sup>Department of Microbiology, University of Washington, Seattle, Washington, USA

## PRESENT ADDRESS

Breah LaSarre, Department of Plant Pathology, Entomology, and Microbiology, Iowa State University, Ames, Iowa, USA

Gina C. Neumann, Benson Hill, St. Louis, Missouri, USA

## AUTHOR ORCIDs

Caroline S. Harwood  <http://orcid.org/0000-0003-4450-5177>

James B. McKinlay  <http://orcid.org/0000-0003-2401-6229>

## FUNDING

Funder	Grant(s)	Author(s)
NSF   BIO   Division of Molecular and Cellular Biosciences (MCB)	MCB-1749489	James B. McKinlay
U.S. Department of Energy (DOE)	DE-FG02-05ER15707	Caroline S. Harwood
U.S. Department of Energy (DOE)	DE-FG02-07ER64482	Caroline S. Harwood

## AUTHOR CONTRIBUTIONS

Breah LaSarre, Investigation, Writing – review and editing | Ryan Morlen, Investigation | Gina C. Neumann, Methodology | Caroline S. Harwood, Funding acquisition, Resources, Writing – review and editing | James B. McKinlay, Conceptualization, Funding acquisition, Investigation, Methodology, Supervision, Writing – original draft, Writing – review and editing

## ADDITIONAL FILES

The following material is available [online](#).

### Supplemental Material

**Table S1 (AEM01741-23-S0001.xlsx).** PSI-BLAST results.

## REFERENCES

1. Zumft WG. 1997. Cell biology and molecular basis of denitrification. *Microbiol Mol Biol Rev* 61:533–616. <https://doi.org/10.1128/mmbr.61.4.533-616.1997>
2. Zumft WG, Kroneck PMH. 2007. Respiratory transformation of nitrous oxide (N<sub>2</sub>O) to dinitrogen by bacteria and archaea. *Adv Microb Physiol* 52:107–227. [https://doi.org/10.1016/S0065-2911\(06\)52003-X](https://doi.org/10.1016/S0065-2911(06)52003-X)
3. Lundberg JO, Weitzberg E, Cole JA, Benjamin N. 2004. Nitrate, bacteria and human health. *Nat Rev Microbiol* 2:593–602. <https://doi.org/10.1038/nrmicro929>
4. Portmann RW, Daniel JS, Ravishankara AR. 2012. Stratospheric ozone depletion due to nitrous oxide: influences of other gases. *Philos Trans R Soc Lond B Biol Sci* 367:1256–1264. <https://doi.org/10.1098/rstb.2011.0377>
5. Barnard R, Leadley PW, Hungate BA. 2005. Global change, nitrification, and denitrification: a review. *Global Biogeochemical Cycles* 19:327–338. <https://doi.org/10.1029/2004GB002282>
6. Reay DS, Davidson EA, Smith KA, Smith P, Melillo JM, Dentener F, Crutzen PJ. 2012. Global agriculture and nitrous oxide emissions. *Nature Clim Change* 2:410–416. <https://doi.org/10.1038/nclimate1458>
7. Roco CA, Bergaust LL, Bakken LR, Yavitt JB, Shapleigh JP. 2017. Modularity of nitrogen-oxide reducing soil bacteria: linking phenotype to genotype. *Environ Microbiol* 19:2507–2519. <https://doi.org/10.1111/1462-2920.13250>
8. Lycus P, Lovise Bøthun K, Bergaust L, Peele Shapleigh J, Reier Bakken L, Frostegård Å. 2017. Phenotypic and genotypic richness of denitrifiers revealed by a novel isolation strategy. *ISME J* 11:2219–2232. <https://doi.org/10.1038/ismej.2017.82>
9. Gowda K, Ping D, Mani M, Kuehn S. 2022. Genomic structure predicts metabolite dynamics in microbial communities. *Cell* 185:530–546. <https://doi.org/10.1016/j.cell.2021.12.036>
10. Graf DRH, Jones CM, Hallin S. 2014. Intergenomic comparisons highlight modularity of the denitrification pathway and underpin the importance of community structure for N<sub>2</sub>O emissions. *PLoS One* 9:e114118. <https://doi.org/10.1371/journal.pone.0114118>
11. Zhang IH, Sun X, Jayakumar A, Fortin SG, Ward BB, Babbin AR. 2023. Partitioning of the denitrification pathway and other nitrite metabolisms within global oxygen deficient zones. *ISME Commun* 3:76. <https://doi.org/10.1038/s43705-023-00284-y>
12. Hallin S, Philippon L, Löffler FE, Sanford RA, Jones CM. 2018. Genomics and ecology of novel N<sub>2</sub>O-reducing microorganisms. *Trends in Microbiology* 26:43–55. <https://doi.org/10.1016/j.tim.2017.07.003>
13. Larimer FW, Chain P, Hauser L, Lamerdin J, Malfatti S, Do L, Land ML, Pelletier DA, Beatty JT, Lang AS, Tabita FR, Gibson JL, Hanson TE, Bobst C, Torres J y, Peres C, Harrison FH, Gibson J, Harwood CS. 2004. Complete genome sequence of the metabolically versatile photosynthetic bacterium *Rhodopseudomonas palustris*. *Nat Biotechnol* 22:55–61. <https://doi.org/10.1038/nbt923>
14. Mazny BE, Sheff OF, LaSarre B, McKinlay A, McKinlay JB. 2023. Complete genome sequence of *Rhodopseudomonas palustris* CGA0092 and corrections to the *R. palustris* CGA009 genome sequence. *Microbiol Resour Announc* 12:e012852. <https://doi.org/10.1128/mra.01285-22>
15. Luxem KE, Kraepiel AML, Zhang L, Waldbauer JR, Zhang X. 2022. Corrigendum: carbon substrate re-orders relative growth of a bacterium using Mo-, V-, or Fe-nitrogenase for nitrogen fixation. *Environ Microbiol* 24:2170–2176. <https://doi.org/10.1111/1462-2920.16001>
16. Luxem KE, Kraepiel AML, Zhang L, Waldbauer JR, Zhang X. 2020. Carbon substrate re-orders relative growth of a bacterium using Mo-, V-, or Fe-nitrogenase for nitrogen fixation. *Environ Microbiol* 22:1397–1408. <https://doi.org/10.1111/1462-2920.14955>
17. Oda Y, Larimer FW, Chain PSG, Malfatti S, Shin MV, Vergez LM, Hauser L, Land ML, Braatsch S, Beatty JT, Pelletier DA, Schaefer AL, Harwood CS. 2008. Multiple genome sequences reveal adaptations of a phototrophic bacterium to sediment microenvironments. *Proc Natl Acad Sci U S A* 105:18543–18548. <https://doi.org/10.1073/pnas.0809160105>
18. Altschul SF, Madden TL, Schäffer AA, Zhang J, Zhang Z, Miller W, Lipman DJ. 1997. Gapped BLAST and PSI-BLAST: a new generation of protein database search programs. *Nucleic Acids Res* 25:3389–3402. <https://doi.org/10.1093/nar/25.17.3389>
19. McKinlay JB, Harwood CS. 2011. Calvin cycle flux, pathway constraints, and substrate oxidation state together determine the H<sub>2</sub> biofuel yield in phototrophic bacteria. *mBio* 2:e00323-10. <https://doi.org/10.1128/mBio.00323-10>
20. Richardson DJ, King GF, Kelly DJ, McEwan AG, Ferguson SJ, Jackson JB. 1988. The role of auxiliary oxidants in maintaining redox balance during phototrophic growth of *Rhodobacter capsulatus* on propionate or butyrate. *Arch. Microbiol* 150:131–137. <https://doi.org/10.1007/BF00425152>
21. Härtig E, Zumft WG. 1999. Kinetics of *nirS* expression (cytochrome cd1 nitrite reductase) in *Pseudomonas stutzeri* during the transition from aerobic respiration to denitrification: evidence for a denitrification-specific nitrate- and nitrite-responsive regulatory system. *J Bacteriol* 181:161–166. <https://doi.org/10.1128/JB.181.1.161-166.1999>
22. Sabaté M, Schwintner C, Cahors S, Richaud P, Verméglio A. 1999. Nitrite and nitrous oxide reductase regulation by nitrogen oxides in *Rhodobacter sphaeroides* f. sp. denitrificans IL106. *J Bacteriol* 181:6028–6032. <https://doi.org/10.1128/JB.181.19.6028-6032.1999>
23. Arai H, Mizutani M, Igarashi Y. 2003. Transcriptional regulation of the nos genes for nitrous oxide reductase in *Pseudomonas aeruginosa*. *Microbiology* 149:29–36. <https://doi.org/10.1099/mic.0.25936-0>
24. Sánchez C, Itakura M, Okubo T, Matsumoto T, Yoshikawa H, Gotoh A, Hidaka M, Uchida T, Minamisawa K. 2014. The nitrate-sensing NasSt system regulates nitrous oxide reductase and periplasmic nitrate reductase in *Bradyrhizobium japonicum*. *Environ Microbiol* 16:3263–3274. <https://doi.org/10.1111/1462-2920.12546>
25. Sánchez C, Mitsui H, Minamisawa K. 2017. Regulation of nitrous oxide reductase genes by NasT-mediated transcription antitermination in *Bradyrhizobium diazoefficiens*. *Environ Microbiol Rep* 9:389–396. <https://doi.org/10.1111/1758-2229.12543>

26. McKinlay JB, Harwood CS. 2010. Carbon dioxide fixation as a central redox Cofactor recycling mechanism in bacteria. *Proc Natl Acad Sci U S A* 107:11669–11675. <https://doi.org/10.1073/pnas.1006175107>

27. McCully AL, Onyeziri MC, LaSarre B, Gliessman JR, McKinlay JB. 2020. Reductive tricarboxylic acid cycle enzymes and reductive amino acid synthesis pathways contribute to electron balance in a *Rhodospirillum rubrum* calvin-cycle mutant. *Microbiology* 166:199–211. <https://doi.org/10.1099/mic.0.000877>

28. Falcone DL, Tabita FR. 1991. Expression of endogenous and foreign ribulose 1,5-bisphosphate carboxylase-oxygenase (RubisCO) genes in a RubisCO deletion mutant of *Rhodobacter sphaeroides*. *J Bacteriol* 173:2099–2108. <https://doi.org/10.1128/jb.173.6.2099-2108.1991>

29. Hallenbeck PL, Lerchen R, Hessler P, Kaplan S. 1990. Roles of CfxA, CfxB, and external electron acceptors in regulation of ribulose 1,5-bisphosphate carboxylase/oxygenase expression in *Rhodobacter sphaeroides*. *J Bacteriol* 172:1736–1748. <https://doi.org/10.1128/jb.172.4.1736-1748.1990>

30. Sánchez C, Itakura M, Mitsui H, Minamisawa K. 2013. Linked expressions of nap and nos genes in a *Bradyrhizobium japonicum* mutant with increased N<sub>2</sub>O reductase activity. *Appl Environ Microbiol* 79:4178–4180. <https://doi.org/10.1128/AEM.00703-13>

31. Cuypers H, Viebrock-Sambale A, Zumft WG. 1992. NosR, a membrane-bound regulatory component necessary for expression of nitrous oxide reductase in denitrifying *Pseudomonas stutzeri*. *J Bacteriol* 174:5332–5339. <https://doi.org/10.1128/jb.174.16.5332-5339.1992>

32. Velasco L, Mesa S, Xu C-A, Delgado MJ, Bedmar EJ. 2004. Molecular characterization of nosRZDFYLX genes coding for denitrifying nitrous oxide reductase of *Bradyrhizobium japonicum*. *Antonie Van Leeuwenhoek* 85:229–235. <https://doi.org/10.1023/B:ANTO.0000020156.42470.db>

33. Cuypers H, Berghöfer J, Zumft WG. 1995. Multiple nosZ promoters and anaerobic expression of nos genes necessary for *Pseudomonas stutzeri* nitrous oxide reductase and assembly of its copper centers. *Biochim Biophys Acta* 1264:183–190. [https://doi.org/10.1016/0167-4781\(95\)00128-4](https://doi.org/10.1016/0167-4781(95)00128-4)

34. Siegel LM, Davis PS, Kamin H. 1974. Reduced nicotinamide adenine dinucleotide phosphate-sulfite reductase of enterobacteria. 3. the *Escherichia coli* hemoflavoprotein: catalytic parameters and the sequence of electron flow. *J Biol Chem* 249:1572–1586.

35. Gaimster H, Alston M, Richardson DJ, Gates AJ, Rowley G. 2018. Transcriptional and environmental control of bacterial denitrification and N<sub>2</sub>O emissions. *FEMS Microbiol Lett* 365:fnx277. <https://doi.org/10.1093/femsle/fnx277>

36. Bergaust L, van Spanning RJM, Frostegård Å, Bakken LR. 2012. Expression of nitrous oxide reductase in *Paracoccus denitrificans* is regulated by oxygen and nitric oxide through Fnlp and Nnr. *Microbiology* 158:826–834. <https://doi.org/10.1099/mic.0.054148-0>

37. Torres MJ, Simon J, Rowley G, Bedmar EJ, Richardson DJ, Gates AJ, Delgado MJ. 2016. Nitrous oxide metabolism in nitrate-reducing bacteria: physiology and regulatory mechanisms. *Adv Microb Physiol* 68:353–432. <https://doi.org/10.1016/bs.ampbs.2016.02.007>

38. Jones CM, Stres B, Rosenquist M, Hallin S. 2008. Phylogenetic analysis of nitrite, nitric oxide, and nitrous oxide respiratory enzymes reveal a complex evolutionary history for denitrification. *Mol Biol Evol* 25:1955–1966. <https://doi.org/10.1093/molbev/msn146>

39. Barth KR, Isabella VM, Clark VL. 2009. Biochemical and genomic analysis of the denitrification pathway within the genus *Neisseria*. *Microbiology* 155:4093–4103. <https://doi.org/10.1099/mic.0.032961-0>

40. Klemme J-H, Chyla I, Preuss M. 1980. Dissimilatory nitrate reduction by strains of the facultative phototrophic bacterium *Rhodopseudomonas palustris*. *FEMS Microbiol Lett* 9:137–140. <https://doi.org/10.1111/j.1574-6968.1980.tb05623.x>

41. McEwan AG, Greenfield AJ, Wetzstein HG, Jackson JB, Ferguson SJ. 1985. Nitrous oxide reduction by members of the family *Rhodospirillaceae* and the nitrous oxide reductase of *Rhodopseudomonas capsulata*. *J Bacteriol* 164:823–830. <https://doi.org/10.1128/jb.164.2.823-830.1985>

42. Rayyan A, Meyer T, Kyndt J. 2018. Draft whole-genome sequence of the purple photosynthetic bacterium *Rhodopseudomonas palustris* XCP. *Microbiol Resour Announc* 7:e00855-18. <https://doi.org/10.1128/MRA.00855-18>

43. Richardson DJ, Bell LC, Moir JWB, Ferguson SJ. 1994. A Denitrifying strain of *Rhodobacter capsulatus*. *FEMS Microbiol Lett* 120:323–328. <https://doi.org/10.1111/j.1574-6968.1994.tb07053.x>

44. Morris JJ, Lenski RE, Zinser ER. 2012. The black queen hypothesis: evolution of dependencies through adaptive gene loss. *mBio* 3:e00036-12. <https://doi.org/10.1128/mBio.00036-12>

45. Lilja EE, Johnson DR. 2016. Segregating metabolic processes into different microbial cells accelerates the consumption of inhibitory substrates. *ISME J* 10:1568–1578. <https://doi.org/10.1038/ismej.2015.243>

46. Perez JC, Groisman EA. 2009. Evolution of transcriptional regulatory circuits in bacteria. *Cell* 138:233–244. <https://doi.org/10.1016/j.cell.2009.07.002>

47. Gordon GC, McKinlay JB. 2014. Calvin cycle mutants of photoheterotrophic purple nonsulfur bacteria fail to grow due to an electron imbalance rather than toxic metabolite accumulation. *J Bacteriol* 196:1231–1237. <https://doi.org/10.1128/JB.01299-13>

48. Rey FE, Oda Y, Harwood CS. 2006. Regulation of uptake hydrogenase and effects of hydrogen utilization on gene expression in *Rhodopseudomonas palustris*. *J Bacteriol* 188:6143–6152. <https://doi.org/10.1128/JB.00381-06>

49. Mesa S, Bedmar EJ, Chanfon A, Hennecke H, Fischer H-M. 2003. *Bradyrhizobium japonicum* NnrR, a denitrification regulator, expands the FixL-FixK2 regulatory cascade. *J Bacteriol* 185:3978–3982. <https://doi.org/10.1128/JB.185.13.3978-3982.2003>

50. Kim M-K, Harwood CS. 1991. Regulation of benzoate-CoA ligase in *Rhodopseudomonas palustris*. *FEMS Microbiol Lett* 83:199–203. <https://doi.org/10.1111/j.1574-6968.1991.tb04440.x-1>

51. Ornston LN. 1966. The conversion of catechol and protocatechuate to beta-ketoadipate by *Pseudomonas putida*. *J Biol Chem* 241:3776–86.

52. Cohen-Bazire G, Sistrom WR, Stanier RY. 1957. Kinetic studies of pigment synthesis by non-sulfur purple bacteria. *J Cell Comp Physiol* 49:25–68. <https://doi.org/10.1002/jcp.1030490104>

53. Huang JJ, Heiniger EK, McKinlay JB, Harwood CS. 2010. Production of hydrogen gas from light and the inorganic electron donor thiosulfate by *Rhodopseudomonas palustris*. *Appl Environ Microbiol* 76:7717–7722. <https://doi.org/10.1128/AEM.01143-10>

54. McCully AL, LaSarre B, McKinlay JB. 2017. Growth-independent cross-feeding modifies boundaries for coexistence in a bacterial mutualism. *Environ Microbiol* 19:3538–3550. <https://doi.org/10.1111/1462-2920.13847>

55. Sauer U, Lasko DR, Fiaux J, Hochuli M, Glaser R, Szyperski T, Wüthrich K, Bailey JE. 1999. Metabolic flux ratio analysis of genetic and environmental modulations of *Escherichia coli* central carbon metabolism. *J Bacteriol* 181:6679–6688. <https://doi.org/10.1128/JB.181.21.6679-6688.1999>

56. McKinlay JB, Shachar-Hill Y, Zeikus JG, Vieille C. 2007. Determining *Actinobacillus succinogenes* metabolic pathways and fluxes by NMR and GC-MS analyses of <sup>13</sup>C-labeled metabolic product isotopomers. *Metab Eng* 9:177–192. <https://doi.org/10.1016/j.ymben.2006.10.006>